The ribotoxin α-sarcin can cleave the sarcin/ricin loop on late 60S pre-ribosomes

Miriam Olombrada[1,2,†], Cohue Peña[2,3,†], Olga Rodríguez-Galán[4,5,†],
Purnima Klingauf-Nerurkar[2,3], Daniela Portugal-Calisto[3], Michaela Oborská-Oplová [2,3],
Martin Altvater[2], José G. Gavilanes[1], Álvaro Martínez-del-Pozo[1], Jesús de la Cruz [4,5,*],
Lucía García-Ortega[1,*] and Vikram Govind Panse [3,*]

[1]Departamento de Bioquímica y Biología Molecular, Facultad de Química, Universidad Complutense de Madrid, Spain, [2]Institute of Biochemistry, ETH Zürich, Otto-Stern-Weg 3, CH-8093 Zürich, Switzerland, [3]Institute of Medical Microbiology, University of Zürich, Gloriastrasse 30, CH-8006 Zürich, Switzerland, [4]Instituto de Biomedicina de Sevilla, Hospital Universitario Virgen del Rocío/CSIC/Universidad de Sevilla, Seville, Spain and [5]Departamento de Genética, Facultad de Biología, Universidad de Sevilla, Seville, Spain

ABSTRACT

The ribotoxin α-sarcin belongs to a family of ribonucleases that cleave the sarcin/ricin loop (SRL), a critical functional rRNA element within the large ribosomal subunit (60S), thereby abolishing translation. Whether α-sarcin targets the SRL only in mature 60S subunits remains unresolved. Here, we show that, in yeast, α-sarcin can cleave SRLs within late 60S pre-ribosomes containing mature 25S rRNA but not nucleolar/nuclear 60S pre-ribosomes containing 27S pre-rRNA *in vivo*. Conditional expression of α-sarcin is lethal, but does not impede early pre-rRNA processing, nuclear export and the cytoplasmic maturation of 60S pre-ribosomes. Thus, SRL-cleaved containing late 60S pre-ribosomes seem to escape cytoplasmic proofreading steps. Polysome analyses revealed that SRL-cleaved 60S ribosomal subunits form 80S initiation complexes, but fail to progress to the step of translation elongation. We suggest that the functional integrity of a α-sarcin cleaved SRL might be assessed only during translation.

INTRODUCTION

The ribosome is an essential ribonucleoprotein complex that translates genetic information into proteins. This universal molecular machine has a conserved two-subunit structure containing rRNAs and ribosomal proteins (r-proteins). In the eukaryotic model organism budding yeast, the small ribosomal subunit (40S), that contains a single 18S rRNA and 33 different r-proteins, is responsible for decoding the genetic information by bringing together mRNAs and tRNAs. The large ribosomal subunit (60S) harbors the peptidyl transferase activity and is composed of three rRNAs (5S, 5.8S and 25S) and 46 r-proteins ([1–3]).

Ribosome assembly is a complex energy consuming process. In eukaryotes, it stretches across the nucleolar, nuclear and cytoplasmic compartments ([4–6]). This process is initiated in the nucleolus with the production of 35S pre-rRNA and 5S RNA by RNA-polymerase I and III, respectively. The pre-rRNA is co-transcriptionally modified and associates with small subunit r-proteins and assembly factors to form the earliest 40S ribosome precursor. Co-transcriptional cleavage releases the earliest 20S pre-rRNA containing 40S pre-ribosome. The remaining emerging pre-rRNA associates with large subunit r-proteins and 60S specific assembly factors to form the early 60S pre-ribosome. 40S pre-ribosomes containing 20S pre-rRNA undergo few compositional changes at the protein level as they travel through the nucleoplasm ([4]). In contrast, 60S pre-ribosomes interact with numerous assembly factors and undergo compositional changes as they travel through the nucleoplasm. The $27SA_2$ pre-rRNA is processed through alternative pathways to 25.5S and $7S_{L/S}$ pre-rRNAs. The nuclear exosome 3′-5′ exonucleolytically processes $7S_{L/S}$ pre-rRNAs to 6S pre-rRNAs and then to mature $5.8S_{L/S}$ rRNAs. In turn, the 25.5S pre-rRNA is 5′-3′ exonucleolytically processed to mature 25S rRNA ([7]).

Correctly assembled pre-ribosomal particles gain export competence and are separately translocated through nuclear pore complexes (NPCs) by multiple FG-interacting transport factors into the cytoplasm (4). Although ribosome assembly is initiated in the nuclear compartment, pre-ribosomes complete maturation only in the cytoplasm. This allows a system of functional checkpoints that ensure only properly matured ribosomal subunits to initiate translation (4,8). The 40S pre-ribosome is accompanied to the cytoplasm by a handful of assembly factors that participate in the Nob1-mediated endonucleolytic cleavage of 20S pre-rRNA into mature 18S rRNA (4,9–11). Although Nob1 associates with the 40S pre-ribosome in the nucleus, its activation occurs only in the cytoplasm, in the context of 40S pre-ribosome or within 80S-like ribosome, which is formed by the joining of a 40S pre-ribosome with a mature 60S subunit (10,12). Nob1 activation appears to require the GTPase activity of the translation initiation factor Fun12/eIF5B and the ATPase activity of the assembly factor Rio1 (10,12,13).

Cytoplasmic maturation of a 60S pre-ribosome involves the sequential release of assembly factors and transport factors, the incorporation of remaining r-proteins and the final trimming of $6S_{L/S}$ pre-rRNAs to mature $5.8S_{L/S}$ rRNAs (14). Release of the assembly factors such as Arx1 that covers the exit tunnel (15,16), the ribosomal-like protein Mrt4 that prevents premature assembly of the acidic stalk r-proteins (uL10/P0, P1 and P2) (17–19) and the anti-association factor Tif6 (20–22) renders a 60S pre-ribosome competent for translation. Genetic trapping and affinity purification combined with targeted proteomic approaches have uncovered additional assembly factors (*e.g.* Bud20, Nsa2, Nug1 and Rli1) that travel with the 60S pre-ribosome to the cytoplasm where they are released (23,24).

Ribotoxins are a family of fungal RNases that catalyze endonucleolytic cleavage of the 23S/25S/28S rRNA at a specific site within the 60S subunit, leading to protein synthesis inhibition and cell death (25). They were originally discovered in the 1960s while screening for antibiotics and antitumor agents (26). Cytotoxicity of these proteins has however limited their clinical use. Recently, ribotoxins have been described as insecticides (27) and components of immunotoxins directed against colon cancer cells (28–30). α-Sarcin was the first ribotoxin described to inhibit protein synthesis *in vitro*. It cleaves a single phosphodiester bond between G_{4325} and A_{4326} of the 28S rRNA within the rat 60S subunit (31,32). This bond is located in the sarcin-ricin loop (SRL), a universally conserved RNA element with an essential role during translation. Ribosomes with a cleaved SRL are unable to activate translational GTPases needed for translation elongation (33). Additionally, the SRL has been hypothesized to activate the GTPase Efl1, resulting in the release of the assembly factor Tif6 (22), to test drive 60S functionality.

While the impact of ribotoxins on translation has been well studied *in vitro*, whether they target the SRL during ribosome assembly remains unclear. Here, we show that only late 60S pre-ribosomes and mature 60S subunits are α-sarcin labile. While α-sarcin expression is lethal, it does not affect export and cytoplasmic maturation of 60S pre-ribosomes. We discuss these results in the context of high-resolution structural information available for dif-

ferent maturation states of 60S pre-ribosomes (14,34,35). Strikingly, SRL cleavage seems to impair the transition from translation initiation to early elongation suggesting that the functional integrity of a SRL may be assessed only later during translation.

MATERIALS AND METHODS

Yeast strains, plasmids and α-sarcin constructs

All recombinant DNA techniques were performed according to established procedures using *Escherichia coli* DH5αF' and XL1-Blue strains for cloning and plasmid propagation. Yeast strains and plasmids used in this study are listed in Supplementary Tables S1 and S2, respectively. All cloned DNA fragments generated by PCR amplification and plasmids were verified by sequencing. Wild type α-sarcin and different mutant variants were cloned under the control of the *GAL1* promoter. For the GFP-tagged α-sarcin constructs, GFP was inserted in the C-terminus of α-sarcin at a *XhoI* restriction site. Wild type fungal α-sarcin was produced and purified from the mold *Aspergillus giganteus* as previously described (36).

In vitro assays of α-sarcin activity

α-Sarcin activity was assayed using cell lysates derived from wild type cells. Briefly, the BY4741 strain was grown in 200 ml of YPD media and harvested at an OD_{600} of 0.75. Cells were washed twice with lysis buffer (30 mM HEPES–NaOH, pH 7.5, 50 mM NaCl, 20 mM $MgCl_2$) and resuspended in 1 ml of lysis buffer. Glass beads were added and cells lysed by vortexing at room temperature and maximum speed for 6 min. The collected lysate was clarified by centrifugation at 14,000 rpm and 4°C for 10 min and concentration of RNA within the lysate was measured. Reactions were performed at 30°C in 25 μl of 30 mM HEPES buffer, pH 7.5 containing 30 mM KCl, 20 mM NaCl, 8 mM $MgCl_2$ and 5 mM β-mercatoethanol for 13 min. 15 μg of RNA containing lysate was supplemented with different concentrations of α-sarcin (0–160 nM). Reactions were stopped by adding Proteinase K to the mix for 15 min at 42°C followed by RNA extraction with phenol–chloroform–isoamyl alcohol and precipitation in isopropanol. RNA pellets were washed with 80% ethanol and resuspended in 15 μl water. 1 μg of total RNA was separated on a 1.2% agarose/formaldehyde gel for 1.5 h at 200 V. RNA was transferred to a nylon membrane (Hybond-N^+; GE Healthcare) by capillary blotting and subsequently UV cross-linked to the membrane (Stratalinker 1800; Agilent Technologies). Northern analyses were performed using 5′-radioactively-labeled probes complementary to the 3′-end sequence of the 25S rRNA (oligo h2, see Supplementary Table S3) and the 5′-end of 27S pre-rRNA (oligo f, see Supplementary Table S3) and visualized using a Phosphorimager screen.

Yeast cell viability assays

Impact of expression of wild type and α-sarcin mutants was analyzed on solid and in liquid growth media. A wild type strain was transformed with an empty plasmid P_{GAL1} or the

constructs P_{GAL1}-SR^{WT} and P_{GAL1}-$SR^{H50/137Q/E96Q}$, which allow expression of wild type α-sarcin or the catalytically inactive H50/137Q/E96Q variant from the *GAL1* promoter, respectively. GFP-tagged version of wild type and mutant α-sarcin were also constructed under the control of *GAL1* promoter and also transformed in the wild type strain. The viability of transformants containing different plasmids with α-sarcin and its mutants were assayed by spotting 10-fold dilutions on glucose- (SD-Ura), or galactose-containing (SG-Ura) plates at 20, 30 and 37°C. For detection of the ribonucleolytic activity *in vivo*, yeast cultures were grown in raffinose-containing media until they reached an OD_{600} of 0.7–0.9. Ribotoxin expression was induced by adding galactose to the culture to a final concentration of 2% (w/v). Culture growth was followed by measuring OD_{600} over time. At different times of induction cells were lysed, RNA was extracted with phenol–chloroform–isoamyl alcohol and results were analyzed by northern blot using a radioactive-labeled probe complementary to the 25S rRNA. For western blot of the GFP-tagged variants, protein extracts were prepared from four units of OD_{600} of the cultures at different times of induction. Briefly, cell pellets were harvested by centrifugation and kept on ice for 5 min. Pellets were then resuspended in 150 µl of solution 1 (1.85 M NaOH, 1.08 M β-mercaptoethanol) and incubated on ice for 10 min. Then, 150 µl of solution 2 (50% TCA) were added to the sample, which was incubated 10 min on ice, followed by centrifugation at 13 000 rpm for 2 min at 4°C. Pellets were resuspended in 1 ml of cold acetone and centrifuged again. Finally, they were resuspended in 100 µl of 1× Laemmli loading buffer. For western blots, 10 µl of each sample were loaded on an SDS/PAGE and analyzed using a GFP specific antibody (dilution 1:2000).

Affinity purification of TAP-tagged proteins

Yeast strains expressing distinct TAP-tagged assembly factors representative of pre-60S particles on the road to mature 60S r-subunits were transformed with either an empty plasmid P_{GAL1} or the construct P_{GAL1}-SR^{WT}. Then, extracts were prepared and used to affinity-purify the different pre-ribosomal particles by IgG-Sepharose beads as previously described (37). Pre-rRNAs co-purifying with these particles were recovered from the beads by phenol–chloroform extraction, as described (38) and assayed by northern hybridization (37). Oligonucleotides (see Supplementary Table S3) were end labelled with 30 µCi [γ-^{32}P]-ATP. Signal intensities were quantified using a FLA-5100 imaging system and Image Gauge (Fujifilm).

Sucrose gradient analyses

Cell extracts for polysome analysis were performed according to Foiani *et al.* (39). Yeast cells harbouring the empty plasmid P_{GAL1} or the constructs P_{GAL1}-SR^{WT} and P_{GAL1}-$SR^{H50/137Q/E96Q}$ were grown at 30°C in raffinose (SR-Ura) and shifted to galactose-containing medium (SG-Ura) for 3 or 8 h. Cultures were harvested at an OD_{600} between 0.5 and 1. Cycloheximide was added to a final concentration of 0.1 mg/ml immediately before harvesting. Cell extracts

were performed, samples equivalent to 10 A_{260} units were layered onto 7–50% linear sucrose gradients and subjected to ultracentrifugation as described by Kressler *et al.* (40). Gradient analyses were performed with an ISCO UV-6 gradient collector and continuously monitored at A_{254}.

To examine the ribonucleolytic activity of α-sarcin in polysome profiles, 0.5 ml aliquots were collected from different fractions of the gradients and RNA was extracted and resuspended in 10 µl of distilled water as described (41). Equal volumes of each fraction were loaded on 7% polyacrylamide containing 8 M urea gels and subjected to northern hybridization (37) as above.

Fluorescence microscopy

uL18-GFP and uS5-GFP based ribosome export assays were performed as previously described (42). α-Sarcin-GFP localization experiments were performed inducing the expression of the toxin for the indicated time points followed by incubation with DAPI 5 µg/ml at 30°C for 30 min. For the localization assays of GFP-tagged versions of the assembly factor Tif6, Mrt4, Arx1, Bud20, Nmd3, Nog1 and Nug1, fluorescence microscopy was done as previously described (23). Cells were visualized using a DM6000B microscope (Leica, Germany) equipped with an HCX PL FluoStar 63×/1.25 NA oil immersion objective (Leica, Solms, Germany). Images were acquired with a fitted digital camera (ORCA-ER; Hamamatsu Photonics, Hamamatsu, SZK, Japan) and analyzed with the Openlab software (Perkin-Elmer, Waltham, MA, USA).

RESULTS

α-Sarcin targets mature 25S rRNA *in vitro*

To investigate substrate specificity of α-sarcin (Figure 1A), we incubated lysates derived from a wild type (WT) budding yeast strain with increasing amounts of the ribotoxin. RNA from the reaction mixtures was isolated, separated on agarose-based electrophoresis and analyzed by northern blot using probes that recognize specific pre-rRNAs and rRNAs. Cleavage of the SRL by α-sarcin was monitored by the appearance of the characteristic small 300-nucleotide fragment of rRNA (α-fragment), that corresponds to the 3′-end of the 25S rRNA, generating simultaneously a large 25S rRNA fragment (25S-α fragment), which is identified below the uncleaved 25S rRNA (43). Consistent with 25S rRNA being an effective substrate of α-sarcin, we found the appearance of these products in a dose dependent manner when yeast lysates were treated with the ribotoxin (Figure 1B). The absence of faster migrating species hybridizing with oligonucleotide f (see Supplementary Table S2) below the intact 27S pre-rRNAs, as well as unaltered 27S pre-rRNA levels with increasing amounts of α-sarcin strongly suggests that ribotoxin targets 25S rRNA, but not the early nucleolar/nuclear 27S precursors (Figure 1B). Thus, the SRL within 27S pre-rRNAs appears not to be efficiently targeted by this ribotoxin. Based on these data, we suggest that 25S rRNA containing 60S pre-ribosomes and mature 60S subunits could be substrates of α-sarcin *in vitro*.
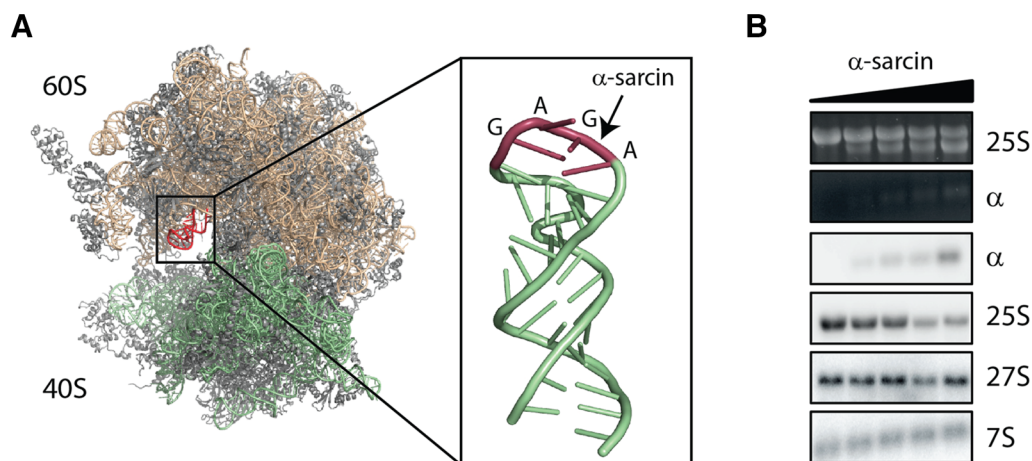
Figure 1. The sarcin-ricin loop (SRL) is targeted by ribotoxins. (**A**) Structure of the eukaryotic ribosome of *S. cerevisiae*. The r-proteins are shown in gray, and rRNAs are shown in colors (18S rRNA in green, 25S, 5.8S and 5S rRNAs in orange). The SRL is shown in red. Inset: Structure of the SRL of *S. cerevisiae* indicating the site of α-sarcin cleavage. Diagrams were generated using PyMOL software (73) (PDB ID: 4V7R; (1)). (**B**) α-Sarcin activity on yeast cell lysates *in vitro*. Total RNA was extracted and analyzed by agarose gel electrophoresis (above, black background panels) and northern blot (below, white background panels) after incubation of the lysate for 13 min with increasing amounts of α-sarcin (0–160 nM). Specific probes for 25S rRNA and 27S pre-rRNA (probes h2 and g, respectively. Supplementary Table S3) were used to detect the cleavage of SRL by northern blot. The probe for 25S rRNA was also used to detect the characteristic fragment released after SRL cleavage (α, for α-fragment).

Conditional expression of α-sarcin in yeast inhibits growth

To investigate the impact of α-sarcin activity *in vivo*, we developed an inducible expression system in budding yeast. Previous attempts to develop a doxycycline inducible expression system resulted in leaky α-sarcin expression that was toxic for yeast even in the absence of induction (44), consistent with previous observations that even few molecules of α-sarcin are lethal (45,46). Therefore, we developed an alternative system that harbors the gene encoding WT α-sarcin under the tight control of the galactose inducible *GAL1* promoter (P_{GAL1}-SR^{WT}). We also included in the study five well characterized α-sarcin variants that exhibit impaired catalytic and/or ribosome recognition activities (P_{GAL1}-SR^{H50Q}, P_{GAL1}-$SR^{H50/137Q}$, P_{GAL1}-$SR^{H50/137Q/E96Q}$, P_{GAL1}-SR^{R121Q}, P_{GAL1}-$SR^{\Delta(7-22)}$) (Figure 2A, summarized in Supplementary Table S4) (47–50). α-Sarcin and its variants were transformed into a WT yeast strain, and the transformants were subsequently grown on repressive glucose-containing solid media. Under these conditions, where expression of α-sarcin and its variants was repressed, yeast cells grew indistinguishably from the WT strain at the three different temperatures tested (Figure 2B). In contrast, on galactose-containing media, growth of yeast was strongly inhibited by WT α-sarcin expression in the entire temperature range from 20°C to 37°C (Figure 2B). Interestingly, the SR^{H50Q} and $SR^{\Delta(7-22)}$ variants, which have a residual non-specific ribonucleolytic activity (Supplementary Table S4), were able to mildly inhibit yeast cell growth at 20°C, but not at higher temperatures (Figure 2B). A slight slow-growth was observed for the catalytically inactive $SR^{H50/137/E96Q}$ mutant, which has been shown to inhibit translation *in vitro* by stoichiometric binding to the ribosome at large doses (51,52).

The deleterious effect of the intracellular expression of α-sarcin on yeast cells is particularly evident in liquid cultures.

Yeast cells from the wild type strain harboring the empty P_{GAL1} plasmid, P_{GAL1}-SR^{WT} or P_{GAL1}-$SR^{H50/137Q/E96Q}$ constructs were grown in repressive raffinose-containing media, and the expression of the toxin induced upon addition of galactose. Upon induction, growth of cells expressing WT α-sarcin was dramatically impaired with noticeable effects even in the initial 60 min, whereas cells expressing the catalytically inactive variant grew at WT rates (Figure 2C).

With this inducible system, we localized α-sarcin and its variants *in vivo* (53). For this, we GFP-tagged either wild type or $SR^{H50/137Q/E96Q}$ α-sarcin and conditionally expressed the resulting fusion proteins in yeast. The chimeric wild type protein maintained its toxicity at any temperature tested (Figure 2D). Next, we assessed the expression levels of wild type and mutant GFP-tagged ribotoxins by western blot using an antibody directed against GFP. As shown in Figure 2E, the fusion construct of the inactive variant ($SR^{H50/137Q/E96Q}$-GFP) could be detected as early as 60 min after induction, whereas the SR^{WT}-GFP protein was only detected after 4 h of induction, in agreement with a delayed growth due to the ribotoxin toxicity. We monitored SR^{WT}-GFP by fluorescence microscopy, inducing the fusion protein for 4 h. As shown in Figure 2F, SR^{WT}-GFP did not enrich in any particular cellular compartment. Instead, it localized to the nucleus and the cytoplasm suggesting that the toxin could attack 60S pre-ribosomes in these compartments.

We investigated the impact of WT α-sarcin activity on ribosome assembly. For this, we isolated total RNA from yeast cells following induction of WT α-sarcin after shifting them from raffinose-containing to galactose-containing media, and assessed the cleavage of the SRL by northern hybridization. As a control, we used yeast cells transformed with the empty P_{GAL1} plasmid. These studies revealed that the SRL within mature 25S rRNA was cleaved
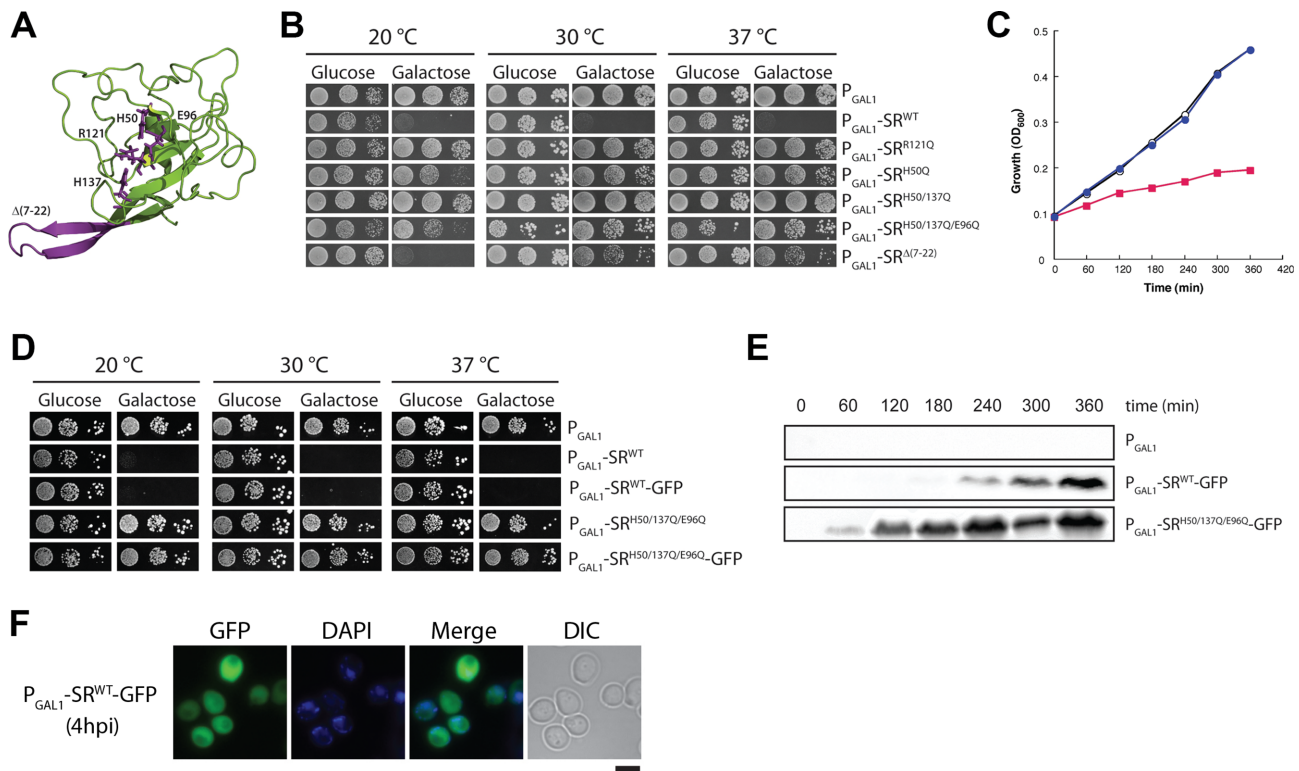
Figure 2. Heterologous expression of ribotoxins in yeast. (**A**) Three-dimensional structure of α-sarcin (PDB ID: 1DE3; (74)) where the deleted sequence and residues changed in the mutants used in this study are highlighted in purple. (**B**) Wild-type yeast cells were transformed with plasmids expressing wild-type α-sarcin (SR^{WT}) or different mutant variants under the control of the *GAL1* promoter. Cells were spotted in 10-fold serial dilutions on plates containing glucose or galactose and grown at the indicated temperatures for 3–6 days. (**C**) Effect of α-sarcin in liquid cultures at 30°C. Wild-type cells expressing wild-type α-sarcin (red squares), the H50/137Q/E96Q inactive variant (blue circles) or transformed with the empty plasmid (black open circles) are depicted in the graph. Expression of α-sarcin was induced by adding 2% galactose (w/v; final concentration) to liquid cultures of SR-Ura medium and the OD$_{600}$ was measured over time. (**D**) Wild-type yeast cells were transformed with plasmids containing wild-type α-sarcin or the H50/137Q/E96Q inactive mutant fused or not to GFP, spotted in 10-fold serial dilutions on plates containing glucose or galactose, and grown at the indicated temperatures for 3–6 days. (**E**) The expression of the GFP-fused proteins at different times of induction was analyzed by western blot using a specific antibody against GFP. Equal amounts of protein extract, equivalent to 0.4 OD$_{600}$ of cells, of each sample were loaded on the gel. (**F**) Intracellular localization of GFP-tagged α-sarcin. Wild-type yeast cells expressing α-sarcin-GFP for 4 h were incubated with 5 μg/ml DAPI for 30 min at 30°C before inspection by fluorescence microscopy. Scale bar = 5 μm.

as judged by the appearance of the α-fragment over time (Figure 3). The amount of α-fragment produced seemed to be constant after 3 h of induction with galactose suggesting a stalling molecular mechanism by α-sarcin during translation (see below). Similar results were previously observed with the doxycycline inducible expression system in yeast, where the extreme toxicity of α-sarcin even selects those cells that have eliminated the ribotoxin-harboring vector (44). As in the case of *in vitro* assays (Figure 1B), the 25S-α fragment could be observed soon upon the induction of α-sarcin (Figure 3), however, neither fragmented 35S pre-rRNA nor fragmented 27S pre-rRNAs could be detected. Altogether, in agreement with previous data (50), our results indicate that the catalytic activity of α-sarcin correlates with its toxicity *in vivo*. Moreover, our data suggest that 35S, 32S and 27S precursors, which all contain the SRL sequence, are not effective substrates of the α-sarcin ribotoxin. Importantly, these data also show that α-sarcin expression does not concomitantly impair pre-rRNA processing.

α-Sarcin does not cleave the SRL within nucle(ol)ar 60S pre-ribosomes

To assess whether α-sarcin is able to cleave the SRL within pre-ribosomes in nuclear and cytoplasmic compartments, we purified pre-ribosomes from WT yeast cells expressing different TAP-tagged bait proteins and P$_{GAL1}$ or the P$_{GAL1}$-SR^{WT}. As baits for nuclear particles, we employed Nop7which is recruited to the 60S pre-ribosome early in the nucleolus and leaves only prior to nuclear export (54). Thus, Nop7-TAP represents a range of early nucleolar to late nuclear 60S pre-ribosomes. Arx1-TAP represents mainly an export competent particle that is loaded with several transport receptors and shuttling assembly factors that travel with the 60S pre-ribosome into the cytoplasm where they are released (23). Replacement of the ribosomal like protein Rlp24 by the r-protein eL24 initiates the cytoplasmic maturation pathway (55). Therefore, eL24-TAP represents both late cytoplasmic 60S pre-ribosomes and mature 60S subunits. Cells were transformed with the P$_{GAL1}$ or the P$_{GAL1}$-SR^{WT} plasmids and grown in galactose-containing media
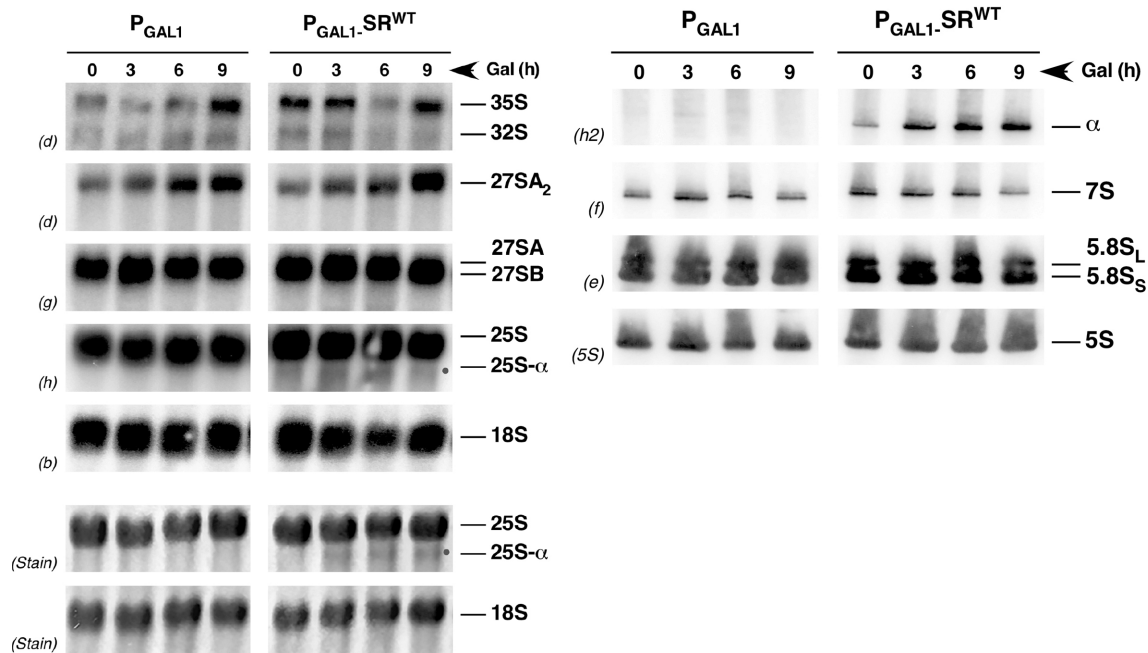
Figure 3. α-Sarcin activity on yeast cell lysates *in vivo*. Wild-type cells expressing wild-type α-sarcin (P_{GAL1}-SR^{WT}) or transformed with the empty plasmid (P_{GAL1}) were grown in liquid SR-Ura medium. Expression of α-sarcin was induced by adding 2% galactose (w/v; final concentration) to the cultures. The OD_{600} of cells was taken at the indicated times and total RNA was extracted. Equal amounts of RNA (5 μg) were analyzed by agarose (left) or acrylamide (right) gel electrophoresis and northern blot. Specific probes were used to detect the different pre- and mature rRNAs as well as the cleavage of SRL by α-sarcin. Panels labelled as 'stain' correspond to the methylene blue staining of the nylon membrane. Black dots denote the 25S-α rRNA fragment. The used probes, in parentheses, are described in Supplementary Figure S1 and Table S3.

for 6 h prior to particle purification. The RNAs were isolated and the precipitated RNAs were analyzed by northern hybridization. As shown in Figure 4, the α-fragment was clearly released only in eL24-TAP and in Arx1-TAP particles isolated from α-sarcin expressing cells. Consistently, the 25S-α fragment could be simultaneously detected in these particles (Figure 4). Importantly, no α-fragment signal above background could be detected when Nop7-TAP containing particles were studied, despite the specific enrichment of 27S pre-rRNAs. Consistent with our previous observation, these studies indicate that the SRL within 27S pre-rRNAs is not targeted by the α-sarcin ribotoxin (Figures 1B and 3).

### α-Sarcin activity does not impair pre-ribosome nuclear export

We wondered whether α-sarcin activity impacts preribosome nuclear export. We monitored the cellular location of known large and small r-subunit reporters (uL18-GFP and uS5-GFP, respectively) after inducing α-sarcin expression in galactose-containing media. As controls, we employed *bud20Δ* and *yrb2Δ* strains that are impaired in the nuclear export of 60S and 40S pre-ribosomes, respectively. While the *bud20Δ* and *yrb2Δ* cells strongly accumulated uL18-GFP and uS5-GFP reporters, respectively, in the nucleus (23,56), yeast cells expressing α-sarcin did not show this phenotype even at longer induction times (Figure 5). As in wild type cells, both reporters localized to the cytoplasm indicating that nucleo-cytoplasmic export of 60S and 40S pre-ribosomes was not compromised upon induction

of the α-sarcin ribotoxin. Importantly, *bud20Δ* and *yrb2Δ* cells expressing α-sarcin still showed a strong nuclear accumulation of both ribosome export reporters, suggesting that these transport assays report nuclear export efficiency in the presence of α-sarcin (Figure 5). These data support the notion that overall ribosome synthesis is not halted and that ample ribosomal proteins are present to drive ribosome production. Therefore, we conclude that α-sarcin activity does not impede nuclear export of pre-ribosomes.

α-Sarcin activity does not impede final maturation of 60S pre-ribosomes

Upon arrival in the cytoplasm, 60S pre-ribosomes undergo final maturation prior to entering translation. These steps involve the sequential release of a subset of assembly factors and transport factors and the incorporation of the last r-proteins (18,42) (Figure 6A). Cytoplasmic maturation is intimately intertwined with ribosome quality control pathways. Defects in assembly and/or function are sensed during these final steps, thereby ensuring that only a correctly assembled subunit completes maturation. The SRL seems to participate in the activation of the GTPase Efl1 and release of the assembly factor Tif6 (22,57). We therefore investigated whether α-sarcin prevents the release and recycling of assembly factors that travel with pre-60S particles to the cytoplasm. P_{GAL1}-SR^{WT} was transformed into different yeast strains in which assembly factors involved in cytoplasmic maturation (Arx1, Bud20, Mrt4, Nmd3, Nog1, Nug1 and Tif6) were fused to GFP at the genomic locus. Localization of the assembly factors was monitored by fluo-
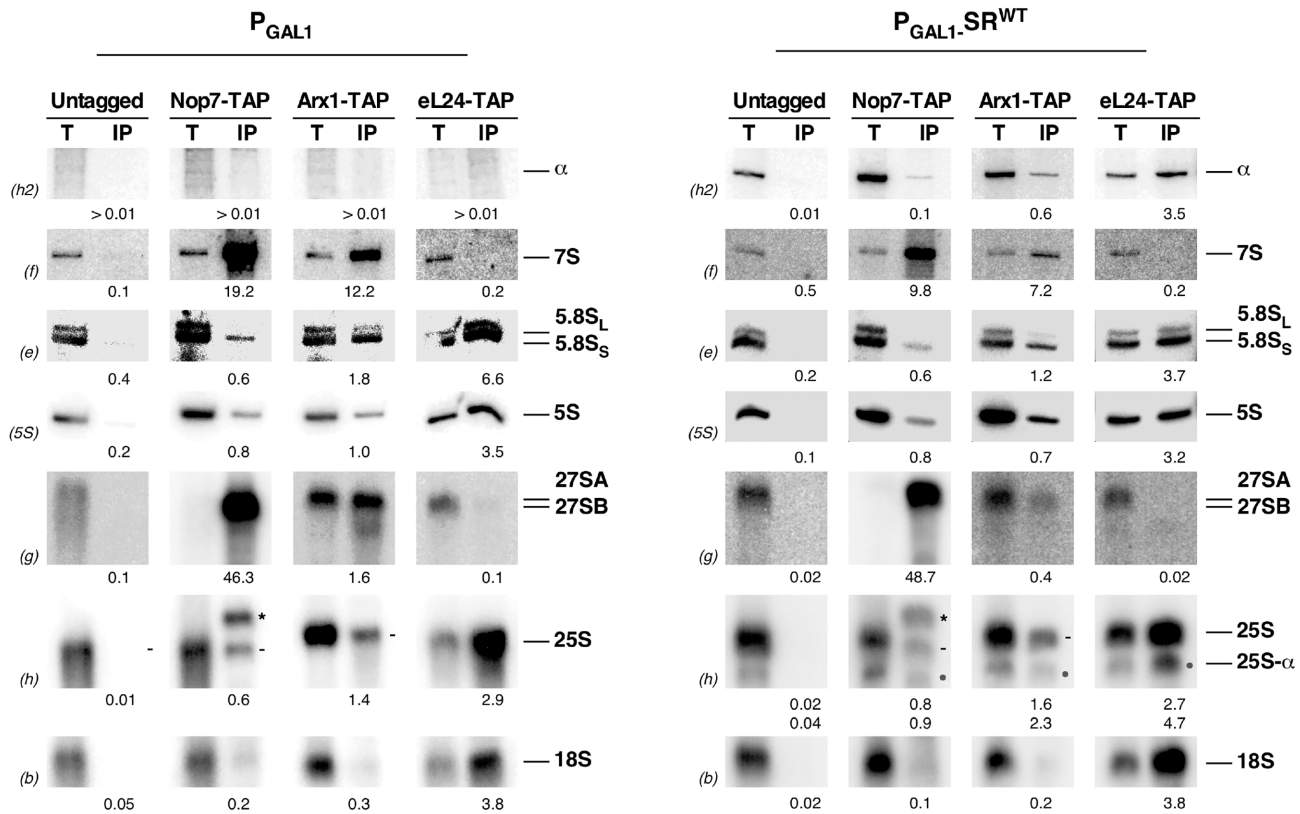
Figure 4. 60S pre-ribosomes containing 27S pre-rRNAs are not targeted by α-sarcin. Isogenic control cells (untagged) or cells expressing TAP-tagged Nop7, Arx1 and eL24A were transformed with an empty plasmid (P$_{GAL1}$) or a plasmid expressing wild-type α-sarcin (P$_{GAL1}$-SR^{WT}) under the control of a *GAL1* promoter. Cells were grown in SR-Ura medium to mid-log phase and then α-sarcin was induced by adding 2% galactose (v/v; final concentration). Immunoprecipitation experiments were carried out using IgG-Sepharose beads and whole-cell extract of the above strains 6 h after the induction of the expression of α-sarcin. RNA was extracted from the beads (lanes IP) or from an amount of total extract corresponding to 1/100 of that used for immunoprecipitation (lanes T), separated on acrylamide (four top panels) or agarose (three bottom panels) gels, transferred to nylon membranes and subjected to northern hybridization with the indicated probes. Black dots denote the 25S-α rRNA fragment, the dash the position of 25S rRNA and the asterisk a contamination of the signal of 27S pre-rRNAs in the membrane. Signal intensities were measured by phosphorimager scanning; values (below each IP lane) refer to the percentage of each RNA recovered after purification. The used probes, between parentheses, are described in Supplementary Figure S1 and Table S3.

rescence microscopy after induction of α-sarcin expression. These studies revealed that inducing α-sarcin activity *in vivo* did not alter the localization of the tested assembly factors (Figure 6B). Based on these data, we suggest that SRL inactivation by α-sarcin did not impede the sequential release of late cytoplasmic assembly factors and therefore, the proper progression of the cytoplasmic maturation pathway.

α-Sarcin activity impairs progression to the translation elongation step

The data until now show that α-sarcin activity did not inhibit nucle(ol)ar assembly, nuclear export and cytoplasmic maturation of ribosomes in yeast. Since the SRL has been strongly implicated in driving translation (33,58), we sought to test whether α-sarcin impairs steps during translation *in vivo*. To this end, cell extracts from wild type cells expressing α-sarcin were prepared under polysome-preserving conditions and analyzed by sucrose gradient centrifugation. The polysomes were then fractionated and subjected to northern analyses. Polysome profiles of lysates derived from cells expressing WT α-sarcin revealed a systematic decrease in the heights of polysome peaks from the di-some to the n-some

in comparison to the catalytically inactive α-sarcin mutant (SR$^{H50/137Q/E96Q}$) and to the empty vector where the peaks did not decrease in heavier fractions (Figure 7A). Northern analyses detected the α-fragment in different fractions (Figure 7B). Quantification of the ratio between α-fragment and mature 5.8S rRNA also revealed a systematic decrease of the former from the monosome to *n*-some fractions (Figure 7C). Based on these data, we suggest that 80S initiation complexes that contain faulty 60S r-subunits with impaired SRLs can assemble onto the mRNAs, but fail to efficiently progress to the elongation phase of translation, thus, stalling early into polysomes.

DISCUSSION

The study of fungal ribotoxins has typically focused on their ability to inactivate mature prokaryotic and/or eukaryotic large ribosomal subunits and to inhibit translation. However, whether mature ribosomes are the only *in vivo* targets of ribotoxins has remained unresolved. The ribosome assembly pathway has been best investigated in the eukaryotic model organism budding yeast that is amenable to genetic, cell-biological and biochemical approaches (4,6). In
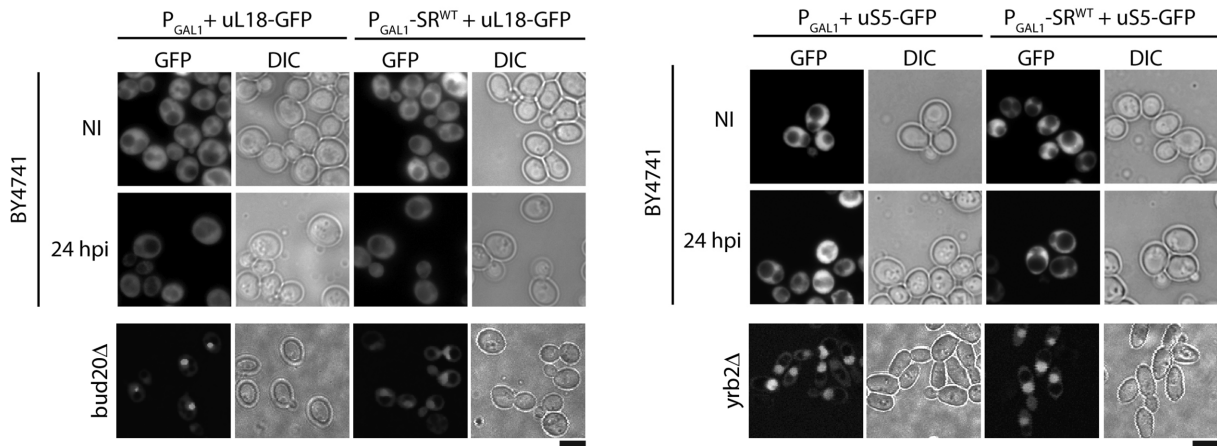
Figure 5. Expression of α-sarcin does not impair nuclear export of 60S pre-ribosomes. Localization of the GFP-tagged uL18 and uS5 r-protein reporters in wild type cells expressing α-sarcin. Cells were grown at 30°C until mid-log phase and then analyzed by fluorescence microscopy before (NI) and 24 h after the induction of ribotoxin expression (24 hpi). Similar results were obtained at shorter induction times. The *bud20Δ* and *yrb2Δ* mutants expressing α-sarcin for 5 h were used as controls for uL18-GFP and uS5-GFP mislocalization, respectively. Scale bar = 5 μm.

this study, we have developed an inducible α-sarcin system in budding yeast that enabled us to investigate the impact of this ribotoxin on the 60S assembly pathway.

In agreement with previous studies in mammalian cells (52), α-sarcin did not enrich/localize to any specific cellular compartment in yeast and can enter the nucleus of cells (Figure 2F), most likely, by passive diffusion across the NPCs due to its small size. This should allow the endonuclease to encounter pre-rRNAs within 60S pre-ribosomes at different maturation stages. Analyses of yeast lysates treated with α-sarcin (Figure 1B) and purified nucleolar pre-60S particles (Nop7-TAP) upon *in vivo* expression of α-sarcin (Figure 4) showed that immature 27S pre-rRNAs could not be cleaved by α-sarcin. In contrast, late nuclear Arx1-TAP particles, cytoplasmic 60S pre-ribosomes and mature 60S r-subunits (eL24-TAP) containing 25S rRNA were substrates for this ribotoxin (Figure 4). Therefore, we conclude that α-sarcin is able to cleave SRLs within both late 60S pre-ribosomes and mature 60S subunits. One explanation for this specificity towards mature 25S rRNA could be that the SRL might not have yet reached its final structure during early maturation to be specifically recognized and cleaved by α-sarcin; however, analysis of the SRL present in distinct pre-60S particles structurally resolved by cryo-electron microscopy (cryo-EM) shows that this scenario is unlikely ((1,59–61), reviewed in (34) and (35); see also Figure 8). Alternatively, the components (e.g. r-proteins that assemble in the cytoplasm) that could be required for α-sarcin recruitment might not be present or in the correct conformation in early 60S pre-ribosomes. Moreover, the SRL might be hindered by particular assembly factors that protect it from the activity of α-sarcin. Recent cryo-EM structures reveal that the assembly factor Nog1 surrounds the tip of the SRL where α-sarcin cleaves, providing a plausible explanation as to why a subset of pre-60S particles are resistant to its enzymatic action (Figure 8). Nog1 associates at an early nucleolar step within 60S pre-ribosomes containing the 27SA₂ pre-rRNA (61,62) and is released shortly after nuclear export of the 60S pre-ribosome ((63); see Figure 6A). Thus,

the SRL seems to be protected by Nog1 during early biogenesis until arrival in the cytoplasm. However, it still remains unclear why the SRL within 27SA₂ pre-rRNA found in very early nucleolar 60S pre-ribosomes (*e.g.* state A in the analysis of Kater *et al.* (61)), which apparently lack Nog1, is resistant to the α-sarcin action. After nuclear export but already during early cytoplasmic maturation, the displacement of the Nog1-G domain presumably through its GTPase activity makes the SRL accessible for cleavage by α-sarcin (Figure 8).

Sucrose gradient sedimentation analyses of lysates derived from yeast cells expressing α-sarcin did not reveal features such as half-mer polysomes that characterize a shortage of 60S subunits (Figure 7A). Moreover, and importantly, α-sarcin expression did neither impair pre-rRNA processing (Figure 3) nor inhibit nuclear export of 60S pre-ribosomes (Figure 5). Upon arrival in the cytoplasm, 60S pre-ribosomes sequentially release assembly factors and transport factors, and acquire remaining r-proteins to form translation-competent 60S subunits (Figure 6A). The release of these factors is carefully regulated, as they appear to assess functionality and prevent the nascent pre-ribosomal particles to engage prematurely into translation (64). Any perturbation in the release of these factors precludes progression of the cytoplasmic maturation pathway. Surprisingly, we found that induction of α-sarcin activity *in vivo* did not impede cytoplasmic maturation of the 60S pre-ribosome (Figure 6B). These data suggest that 60S pre-ribosomes with cleaved SRLs evade cytoplasmic proofreading mechanisms. The SRL loop has been directly implicated in activation of translational GTPase activity during polypeptide elongation (65–67). Given its critical importance during translation, the folding and integrity of SRL is expected to require close monitoring during 60S subunit assembly. Tif6 is one of the proofreading factors that prevents incorrectly assembled 60S pre-ribosomes from completing final maturation and entering into the translation cycle (18). The SRL within 60S pre-ribosomes has been suggested to activate the GTPase Efl1 activity to orchestrate re-
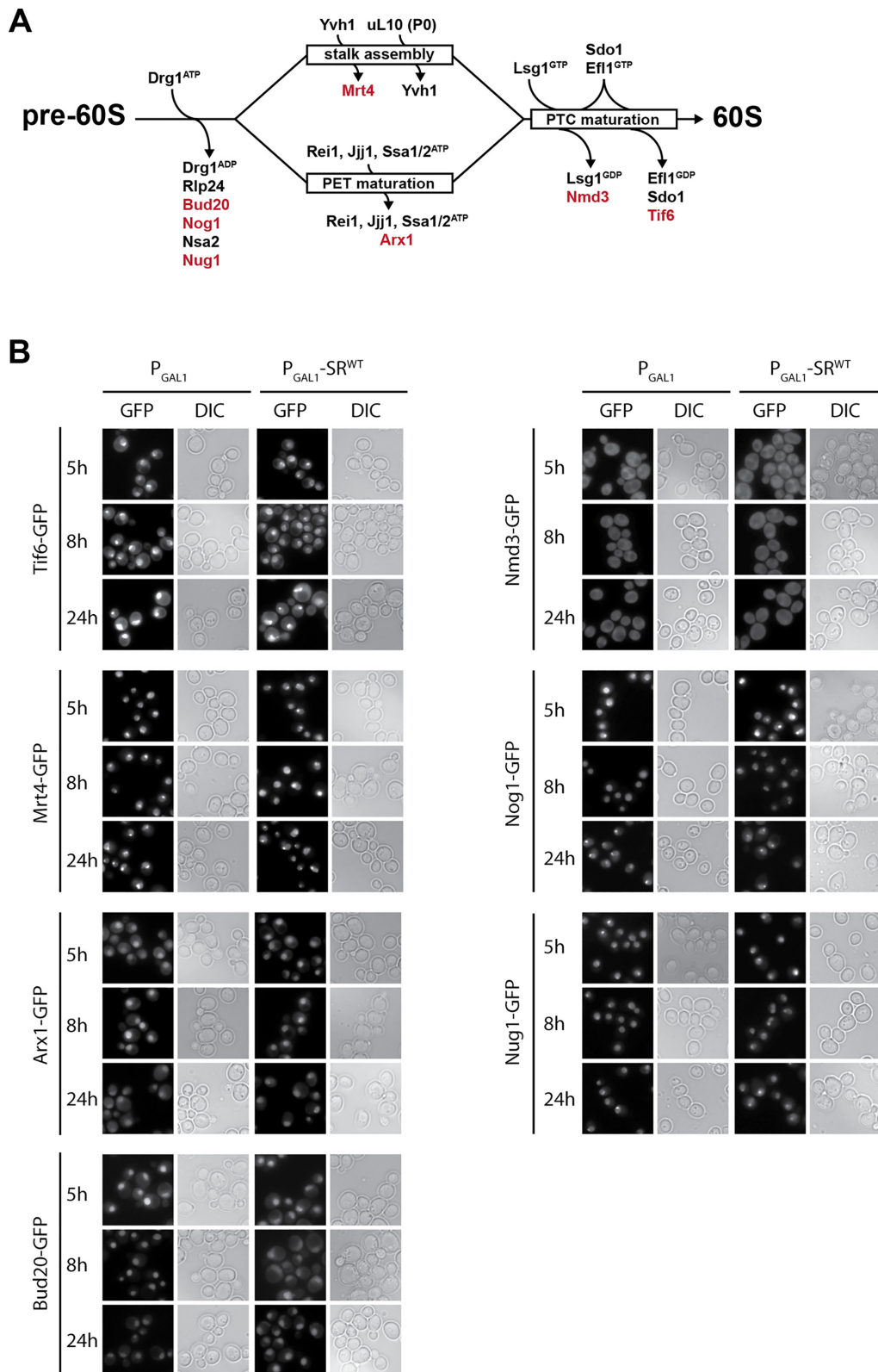
Figure 6. Location of shuttling assembly factors upon induction of α-sarcin expression. (**A**) Proposed pathway of 60S r-subunit maturation in the cytoplasm (adapted from (24)). The assembly factors analyzed in (**B**) are shown in red. (**B**) Recycling of nucleo-cytoplasmic shuffling *trans*-acting factors is not affected by the α-sarcin expression. Yeast strains expressing different GFP-tagged *trans*-acting factors (Tif6, Mrt4, Arx1, Bud20, Nmd3, Nog1, Nug1) were transformed with the vector containing wild-type α-sarcin (P$_{GAL1}$-SR^{WT}) or an empty control plasmid (P$_{GAL1}$). Intracellular localization of these factors was analyzed by fluorescence microscopy 5, 8 and 24 h after the induction of the ribotoxin expression. Scale bar = 5 μm.
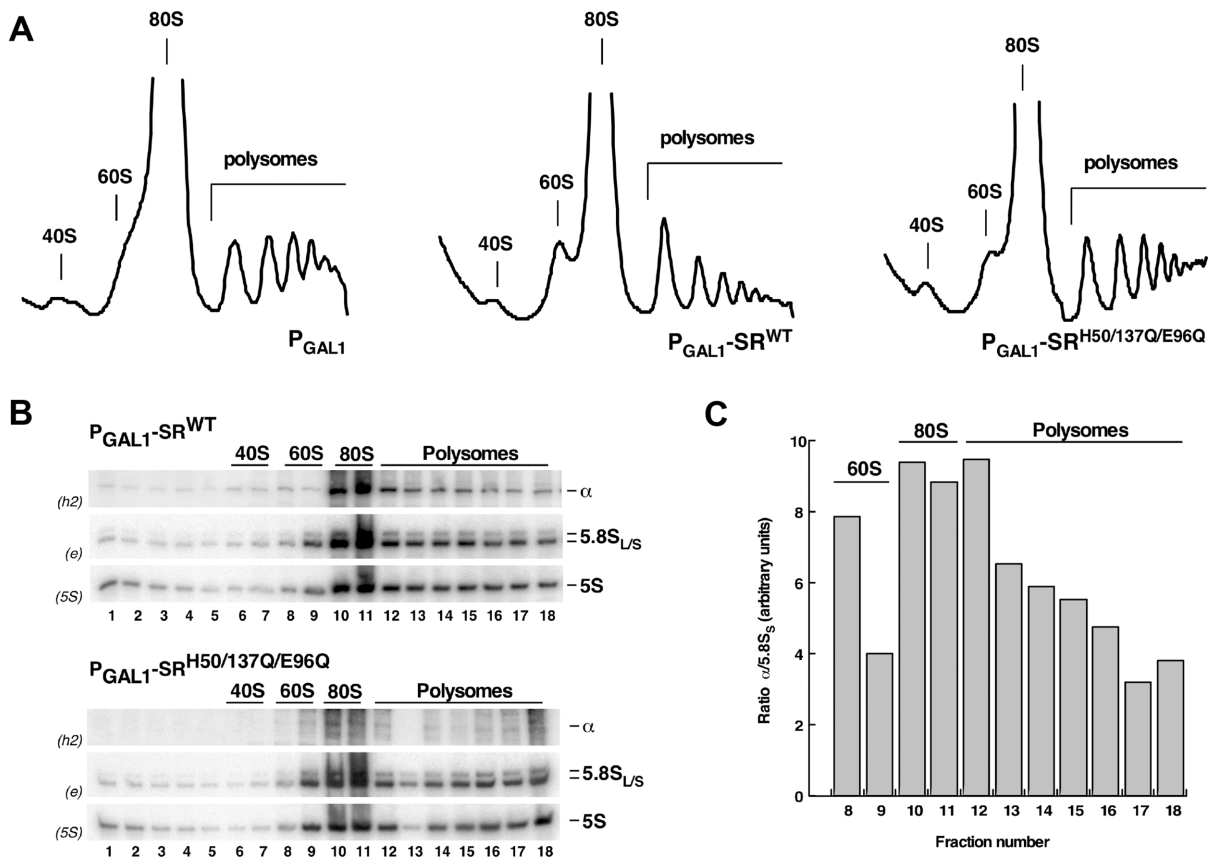
Figure 7. Expression of α-sarcin affects translation elongation in yeast. (**A**) Sucrose gradient profiles of wild-type yeast cells transformed with an empty P_{GAL1}, P_{GAL1}-SR^{WT} or P_{GAL1}-$SR^{H50/137Q/E96Q}$ plasmid, grown in SR-Ura medium and shifted for 4 h to SG-Ura medium. The peaks of free 40S and 60S r-subunits, 80S and polysomes are indicated. (**B**) Detection of the α-fragment (α) produced by α-sarcin in the different fractions by northern blot. The used probes, in parentheses, are described in Supplementary Figure S1 and Table S3. (**C**) Quantification of the ratio α/5.8S rRNA (arbitrary units) when wild type α-sarcin expression is induced.

lease of the assembly factor Tif6 (22). In this way, integrity of the SRL is thought to be functionally tested to permit progression of pre-ribosome maturation. In agreement with this model, structural studies have revealed several contacts between domain III of Efl1 and the SRL (22). However, whether or not an intact SRL is required for Efl1 activation has not been directly tested. One prediction would be that a cytoplasmic 60S pre-ribosome with a cleaved SRL would fail to release and recycle Tif6 back to the nucleus. Surprisingly, we found that this was not the case as Tif6 localization remained unaltered upon inducing α-sarcin activity *in vivo* (Figure 6B). It could be that a different mechanism might be operating to activate GTPase activity of Efl1 to release Tif6 from the cytoplasmic 60S pre-ribosome or that, unlike translational GTPases, a cleaved SRL is still competent to activate Efl1 for Tif6 release. It is well-established that SRL cleavage does differently affect EF-Tu and EF-G binding and functionality (33), thus making likely the latter possibility.

The data presented here strongly suggest that 60S pre-ribosomes with cleaved SRLs undergo final maturation yielding non-functional 60S subunits that are unable to properly translate. Polysome analyses revealed similar levels of 80S monosomes in cells expressing WT α-sarcin as compared to cells expressing either an empty vector or the cat-

alytically inactive α-sarcin mutant ($SR^{H50/137Q/E96Q}$). However, we observed a marked reduction of polysome peaks in lysates derived from cells expressing WT α-sarcin (Figure 7A). Polysome profiles of lysates derived from cells expressing α-sarcin do not represent a translation initiation defect, which should occur through an increase in the peak of 80S. Instead, these profiles revealed a systematic decrease in the heights of polysome peaks from the disome to the n-some, which is not occurring in those profiles derived from cells expressing the catalytically inactive α-sarcin mutant ($SR^{H50/137Q/E96Q}$) or transformed with the empty vector (Figure 7A). Northern analyses detected the α-fragment in different fractions (Figure 7B). Quantification of the ratio between α-fragment and mature 5.8S rRNA also revealed a systematic decrease of the former from the monosome to n-some fractions (Figure 7C). This corresponds to a mRNA covered by several ribosomes before the last 60S subunit, containing a cleaved SRL, joins the polysome forming a non-functional 80S ribosome, which stops translation. Based on these data, we suggest that 80S initiation complexes that contain a faulty 60S subunit with an impaired SRL can assemble onto a mRNA, but fails to progress to the elongation phase of translation, thus, stalling further formation of polysomes. If a translation initiation defect was occurring, i.e. recruitment of the 60S sub-
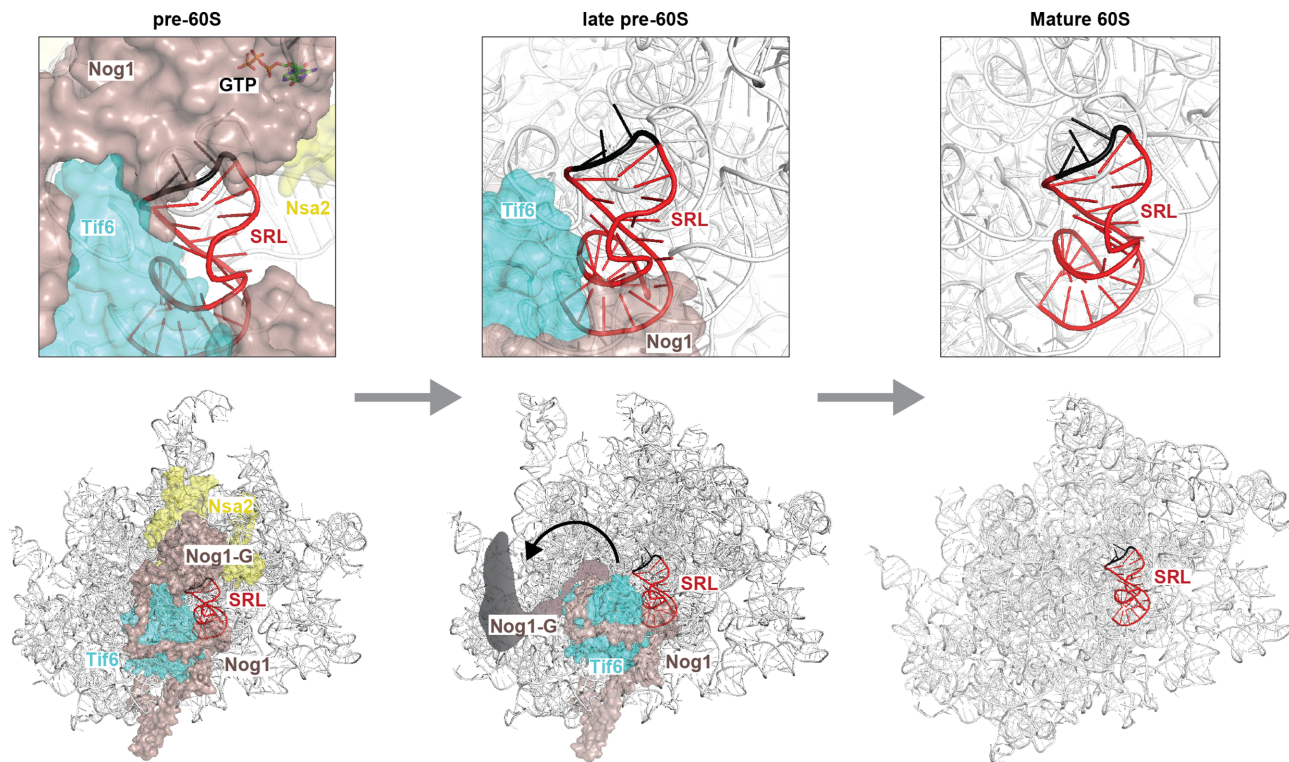
Figure 8. Accessibility of the SRL in different 60S pre-ribosomes. Nuclear late 60S pre-ribosome (PDB ID: 3JCT; (59)), cytoplasmic 60S pre-ribosome (PDB ID: 6N8L; (75)) and a mature 60S subunit (PDB ID: 4V7R; (1)) were generated by PyMOL (73). The SRL is represented in red with the cleavage sequence in black. The assembly factors Nog1, Nsa2 and Tif6 are represented in brown, yellow and blue respectively.

unit was impaired, the alpha fragment should not be detected in polysome fractions but only in the 80S peak corresponding to vacant 80S ribosomes (Figure 7C). This is also consistent with the fact that the SRL plays a crucial role in translation elongation (65–67). Thus, the result of α-sarcin activity appears to go unnoticed by quality control mechanisms that check the integrity of the 60S r-subunit. This can inhibit protein synthesis and induce cell death. We suggest that the functionality of an α-sarcin cleaved SRL might not be assessed during 60S subunit maturation.

Another group of toxic proteins that also target the ribosomal SRL includes ricin, bacterial Shiga toxins (Stx1 and Stx2) and the pokeweed antiviral protein. These ribosome-inactivating proteins exhibit N-glycosidase activity to depurinate an universally conserved adenine base within the SRL (68). Depurination of the SRL also interferes with the binding of translation elongation factors (69). However, recently, it has suggested that, at least in yeast, the main source of ricin toxicity is not the inhibition of the translational machinery (70). Interestingly, these toxins employ the 60S r-stalk as a docking platform to access and depurinate the SRL (71,72). Thus, 60S pre-ribosomes which have not yet assembled the stalk in the cytoplasm may be resistant to these class of ribotoxins (71,72). In the case of ribotoxins like α-sarcin, the presence of the r-stalk is not needed for its cytotoxicity (44). Consistent with this, we show that 60S pre-ribosomes that contain mature 25S rRNA but have not yet assembled an r-stalk (*e.g.* Arx1-TAP containing particles) are still efficient substrates of α-sarcin (Figure 4).

A particular barrier to investigate the impact of ribotoxins *in vivo* is their inherent toxicity. Here, an inducible heterologous expression system in budding yeast allowed tight control of α-sarcin expression. Given the diverse biochemical and proteomic tools amenable in budding yeast as a model organism, this system can now be exploited to study the consequences of ribotoxin mediated translation inhibition on different cellular pathways, and therefore uncover the underlying basis for their toxicity.

DEDICATIONS

This article is dedicated to the memory of Dr. Cohue Peña, who unfortunately passed away during the course of this study.

SUPPLEMENTARY DATA

Supplementary Data are available at NAR Online.

FUNDING

REFERENCES

1. Ben-Shem,A., Garreau de Loubresse,N., Melnikov,S., Jenner,L., Yusupova,G. and Yusupov,M. (2011) The structure of the eukaryotic ribosome at 3.0 A resolution. *Science*, **334**, 1524–1529.
2. Klinge,S., Voigts-Hoffmann,F., Leibundgut,M., Arpagaus,S. and Ban,N. (2011) Crystal structure of the eukaryotic 60S ribosomal subunit in complex with initiation factor 6. *Science*, **334**, 941–948.
3. Rabl,J., Leibundgut,M., Ataide,S.F., Haag,A. and Ban,N. (2011) Crystal structure of the eukaryotic 40S ribosomal subunit in complex with initiation factor 1. *Science*, **331**, 730–736.
4. Gerhardy,S., Menet,A.M., Peña,C., Petkowski,J.J. and Panse,V.G. (2014) Assembly and nuclear export of pre-ribosomal particles in budding yeast. *Chromosoma*, **123**, 327–344.
5. Nerurkar,P., Altvater,M., Gerhardy,S., Schütz,S., Fischer,U., Weirich,C. and Panse,V.G. (2015) Eukaryotic ribosome assembly and nuclear export. *Int. Rev. Cell Mol. Biol.*, **319**, 107–140.
6. Woolford,J.L. Jr. and Baserga,S.J. (2013) Ribosome biogenesis in the yeast *Saccharomyces cerevisiae. Genetics*, **195**, 643–681.
7. Fernández-Pevida,A., Kressler,D. and de la Cruz,J. (2015) Processing of preribosomal RNA in *Saccharomyces cerevisiae. Wiley Interdiscip. Rev. RNA*, **6**, 191–209.
8. Greber,B.J., Gerhardy,S., Leitner,A., Leibundgut,M., Salem,M., Boehringer,D., Leulliot,N., Aebersold,R., Panse,V.G. and Ban,N. (2016) Insertion of the biogenesis factor Rei1 probes the ribosomal tunnel during 60S maturation. *Cell*, **164**, 91–102.
9. Pertschy,B., Schneider,C., Gnadig,M., Schafer,T., Tollervey,D. and Hurt,E. (2009) RNA helicase Prp43 and its co-factor Pfa1 promote 20 to 18 S rRNA processing catalyzed by the endonuclease Nob1. *J. Biol. Chem.*, **284**, 35079–35091.
10. Strunk,B.S., Novak,M.N., Young,C.L. and Karbstein,K. (2012) A translation-like cycle is a quality control checkpoint for maturing 40S ribosome subunits. *Cell*, **150**, 111–121.
11. Cerezo,E., Plisson-Chastang,C., Henras,A.K., Lebaron,S., Gleizes,P.E., O'Donohue,M.F., Romeo,Y. and Henry,Y. (2019) Maturation of pre-40S particles in yeast and humans. *Wiley Interdiscip. Rev. RNA*, **10**, e1516.
12. Turowski,T.W., Lebaron,S., Zhang,E., Peil,L., Dudnakova,T., Petfalski,E., Granneman,S., Rappsilber,J. and Tollervey,D. (2014) Rio1 mediates ATP-dependent final maturation of 40S ribosomal subunits. *Nucleic. Acids. Res.*, **42**, 12189–12199.
13. Lebaron,S., Schneider,C., van Nues,R.W., Swiatkowska,A., Walsh,D., Bottcher,B., Granneman,S., Watkins,N.J. and Tollervey,D. (2012) Proofreading of pre-40S ribosome maturation by a translation initiation factor and 60S subunits. *Nat. Struct. Mol. Biol.*, **19**, 744–753.
14. Peña,C., Hurt,E. and Panse,V.G. (2017) Eukaryotic ribosome assembly, transport and quality control. *Nat. Struct. Mol. Biol.*, **24**, 689–699.
15. Hung,N.J. and Johnson,A.W. (2006) Nuclear recycling of the pre-60S ribosomal subunit-associated factor Arx1 depends on Rei1 in *Saccharomyces cerevisiae. Mol. Cell. Biol.*, **26**, 3718–3727.
16. Lebreton,A., Saveanu,C., Decourty,L., Rain,J.C., Jacquier,A. and Fromont-Racine,M. (2006) A functional network involved in the recycling of nucleocytoplasmic pre-60S factors. *J. Cell Biol.*, **173**, 349–360.
17. Kemmler,S., Occhipinti,L., Veisu,M. and Panse,V.G. (2009) Yvh1 is required for a late maturation step in the 60S biogenesis pathway. *J. Cell Biol.*, **186**, 863–880.
18. Lo,K.Y., Li,Z., Bussiere,C., Bresson,S., Marcotte,E.M. and Johnson,A.W. (2010) Defining the pathway of cytoplasmic maturation of the 60S ribosomal subunit. *Mol. Cell*, **39**, 196–208.
19. Rodríguez-Mateos,M., García-Gómez,J.J., Francisco-Velilla,R., Remacha,M., de la Cruz,J. and Ballesta,J.P.G. (2009) Role and dynamics of the ribosomal protein P0 and its related *trans*-acting factor Mrt4 during ribosome assembly in *Saccharomyces cerevisiae. Nucleic Acids Res.*, **37**, 7519–7532.
20. Menne,T.F., Goyenechea,B., Sanchez-Puig,N., Wong,C.C., Tonkin,L.M., Ancliff,P.J., Brost,R.L., Costanzo,M., Boone,C. and Warren,A.J. (2007) The Shwachman-Bodian-Diamond syndrome protein mediates translational activation of ribosomes in yeast. *Nat. Genet.*, **39**, 486–495.
21. Senger,B., Lafontaine,D.L., Graindorge,J.S., Gadal,O., Camasses,A., Sanni,A., Garnier,J.M., Breitenbach,M., Hurt,E. and Fasiolo,F. (2001) The nucle(ol)ar Tif6p and Efl1p are required for a late cytoplasmic step of ribosome synthesis. *Mol. Cell*, **8**, 1363–1373.
22. Weis,F., Giudice,E., Churcher,M., Jin,L., Hilcenko,C., Wong,C.C., Traynor,D., Kay,R.R. and Warren,A.J. (2015) Mechanism of eIF6 release from the nascent 60S ribosomal subunit. *Nat. Struct. Mol. Biol.*, **22**, 914–919.
23. Altvater,M., Chang,Y., Melnik,A., Occhipinti,L., Schütz,S., Rothenbusch,U., Picotti,P. and Panse,V.G. (2012) Targeted proteomics reveals compositional dynamics of 60S pre-ribosomes after nuclear export. *Mol. Syst. Biol.*, **8**, 628.
24. Klingauf-Nerurkar,P., Gillet,L.C., Portugal-Calisto,D., Oborská-Oplová,M., Jäger,M., Schubert,O.T., Pisano,A., Peña,C., Rao,S., Altvater,M. *et al.* (2020) The GTPase Nog1 co-ordinates the assembly, maturation and quality control of distant ribosomal functional centers. *eLife*, **9**, e52474.
25. Lacadena,J., Álvarez-García,E., Carreras-Sangrà,N., Herrero-Galán,E., Alegre-Cebollada,J., García-Ortega,L., Oñaderra,M., Gavilanes,J.G. and Martínez del Pozo,A. (2007) Fungal ribotoxins: molecular dissection of a family of natural killers. *FEMS Microbiol. Rev.*, **31**, 212–237.
26. Olson,B.H. and Goerner,G.L. (1965) Alpha sarcin, a new antitumor agent. i. isolation, purification, chemical composition, and the identity of a new amino acid. *Appl. Microbiol.*, **13**, 314–321.
27. Olombrada,M., Martínez-del-Pozo,A., Medina,P., Budia,F., Gavilanes,J.G. and García-Ortega,L. (2014) Fungal ribotoxins: Natural protein-based weapons against insects. *Toxicon*, **83**, 69–74.
28. Tomé-Amat,J., Herrero-Galán,E., Oñaderra,M., Martínez-Del-Pozo,A., Gavilanes,J.G. and Lacadena,J. (2015) Preparation of an engineered safer immunotoxin against colon carcinoma based on the ribotoxin hirsutellin A. *FEBS J.*, **282**, 2131–2141.
29. Tomé-Amat,J., Olombrada,M., Ruiz-de-la-Herrán,J., Pérez-Gómez,E., Andradas,C., Sánchez,C., Martínez,L., Martínez-Del-Pozo,A., Gavilanes,J.G. and Lacadena,J. (2015) Efficient *in vivo* antitumor effect of an immunotoxin based on ribotoxin alpha-sarcin in nude mice bearing human colorectal cancer xenografts. *Springerplus*, **4**, 168.
30. Tomé-Amat,J., Ruiz-de-la-Herrán,J., Martínez-del-Pozo,A., Gavilanes,J.G. and Lacadena,J. (2015) alpha-sarcin and RNase T1 based immunoconjugates: the role of intracellular trafficking in cytotoxic efficiency. *FEBS J.*, **282**, 673–684.
31. Endo,Y. and Wool,I.G. (1982) The site of action of alpha-sarcin on eukaryotic ribosomes. The sequence at the alpha-sarcin cleavage site in 28 S ribosomal ribonucleic acid. *J. Biol. Chem.*, **257**, 9054–9060.
32. Schindler,D.G. and Davies,J.E. (1977) Specific cleavage of ribosomal RNA caused by alpha sarcin. *Nucleic Acids Res.*, **4**, 1097–1110.
33. García-Ortega,L., Álvarez-García,E., Gavilanes,J.G., Martínez-del-Pozo,A. and Joseph,S. (2010) Cleavage of the sarcin-ricin loop of 23S rRNA differentially affects EF-G and EF-Tu binding. *Nucleic Acids Res.*, **38**, 4108–4119.
34. Bassler,J. and Hurt,E. (2019) Eukaryotic ribosome assembly. *Annu. Rev. Biochem.*, **88**, 281–306.
35. Kressler,D., Hurt,E. and Bassler,J. (2017) A puzzle of life: crafting ribosomal subunits. *Trends Biochem. Sci.*, **42**, 640–654.
36. Lacadena,J., Martínez del Pozo,A., Barbero,J.L., Mancheño,J.M., Gasset,M., Oñaderra,M., López-Otín,C., Ortega,S., García,J. and Gavilanes,J.G. (1994) Overproduction and purification of biologically active native fungal alpha-sarcin in *Escherichia coli. Gene*, **142**, 147–151.
37. Rodríguez-Galán,O., García-Gómez,J.J., Kressler,D. and de la Cruz,J. (2015) Immature large ribosomal subunits containing the 7S pre-rRNA can engage in translation in *Saccharomyces cerevisiae. RNA Biol.*, **12**, 838–846.
38. Lebaron,S., Froment,C., Fromont-Racine,M., Rain,J.C., Monsarrat,B., Caizergues-Ferrer,M. and Henry,Y. (2005) The splicing ATPase Prp43p is a component of multiple preribosomal particles. *Mol. Cell. Biol.*, **25**, 9269–9282.

39. Foiani,M., Cigan,A.M., Paddon,C.J., Harashima,S. and Hinnebusch,A.G. (1991) GCD2, a translational repressor of the *GCN4* gene, has a general function in the initiation of protein synthesis in *Saccharomyces cerevisiae*. *Mol. Cell. Biol.*, **11**, 3203–3216.

40. Kressler,D., de la Cruz,J., Rojo,M. and Linder,P. (1997) Fal1p is an essential DEAD-box protein involved in 40S-ribosomal-subunit biogenesis in *Saccharomyces cerevisiae*. *Mol. Cell. Biol.*, **17**, 7283–7294.

41. de la Cruz,J., Kressler,D., Rojo,M., Tollervey,D. and Linder,P. (1998) Spb4p, an essential putative RNA helicase, is required for a late step in the assembly of 60S ribosomal subunits in *Saccharomyces cerevisiae*. *RNA*, **4**, 1268–1281.

42. Altvater,M., Schütz,S., Chang,Y. and Panse,V.G. (2014) Dissecting ribosome assembly and transport in budding yeast. *Methods Cell Biol.*, **122**, 437–461.

43. Schindler,D.G. and Davies,J.E. (1977) Specific cleavage of ribosomal RNA caused by alpha sarcin. *Nucleic Acids Res.*, **4**, 1097–1110.

44. Olombrada,M., Rodríguez-Mateos,M., Prieto,D., Pla,J., Remacha,M., Martínez-del-Pozo,A., Gavilanes,J.G., Ballesta,J.P. and García-Ortega,L. (2014) The acidic ribosomal stalk proteins are not required for the highly specific inactivation exerted by alpha-sarcin of the eukaryotic ribosome. *Biochemistry*, **53**, 1545–1547.

45. Lamy,B., Davies,J. and Schindler,D. (1992) The *Aspergillus* ribonucleolytic toxins (ribotoxins). *Targeted Diagn. Ther.*, **7**, 237–258.

46. Yang,R. and Kenealy,W.R. (1992) Effects of amino-terminal extensions and specific mutations on the activity of restrictocin. *J. Biol. Chem.*, **267**, 16801–16805.

47. García-Mayoral,M.F., García-Ortega,L., Lillo,M.P., Santoro,J., Martínez del Pozo,A., Gavilanes,J.G., Rico,M. and Bruix,M. (2004) NMR structure of the noncytotoxic alpha-sarcin mutant Delta(7-22): the importance of the native conformation of peripheral loops for activity. *Protein Sci.*, **13**, 1000–1011.

48. García-Ortega,L., Masip,M., Mancheño,J.M., Oñaderra,M., Lizarbe,M.A., García-Mayoral,M.F., Bruix,M., Martínez del Pozo,A. and Gavilanes,J.G. (2002) Deletion of the NH₂-terminal beta-hairpin of the ribotoxin alpha-sarcin produces a nontoxic but active ribonuclease. *J. Biol. Chem.*, **277**, 18632–18639.

49. Lacadena,J., Martínez del Pozo,A., Martínez-Ruiz,A., Pérez-Canadillas,J.M., Bruix,M., Mancheño,J.M., Oñaderra,M. and Gavilanes,J.G. (1999) Role of histidine-50, glutamic acid-96, and histidine-137 in the ribonucleolytic mechanism of the ribotoxin alpha-sarcin. *Proteins*, **37**, 474–484.

50. Masip,M., Lacadena,J., Mancheño,J.M., Onaderra,M., Martínez-Ruiz,A., Martínez del Pozo,A. and Gavilanes,J.G. (2001) Arginine 121 is a crucial residue for the specific cytotoxic activity of the ribotoxin alpha-sarcin. *Eur. J. Biochem.*, **268**, 6190–6196.

51. Álvarez-García,E., Diago-Navarro,E., Herrero-Galán,E., García-Ortega,L., López-Villarejo,J., Olmo,N., Díaz-Orejas,R., Gavilanes,J.G. and Martínez-del-Pozo,A. (2011) The ribonucleolytic activity of the ribotoxin alpha-sarcin is not essential for in vitro protein biosynthesis inhibition. *Biochim. Biophys. Acta*, **1814**, 1377–1382.

52. Alford,S.C., Pearson,J.D., Carette,A., Ingham,R.J. and Howard,P.L. (2009) Alpha-sarcin catalytic activity is not required for cytotoxicity. *BMC Biochem.*, **10**, 9.

53. Enterina,J.R., Wu,L. and Campbell,R.E. (2015) Emerging fluorescent protein technologies. *Curr. Opin. Chem. Biol.*, **27**, 10–17.

54. Kressler,D., Roser,D., Pertschy,B. and Hurt,E. (2008) The AAA ATPase Rix7 powers progression of ribosome biogenesis by stripping Nsa1 from pre-60S particles. *J. Cell Biol.*, **181**, 935–944.

55. Lo,K.Y., Li,Z., Bussiere,C., Bresson,S., Marcotte,E.M. and Johnson,A.W. (2010) Defining the pathway of cytoplasmic maturation of the 60S ribosomal subunit. *Mol. Cell*, **39**, 196–208.

56. Moy,T.I. and Silver,P.A. (2002) Requirements for the nuclear export of the small ribosomal subunit. *J. Cell Sci.*, **115**, 2985–2995.

57. Bussiere,C., Hashem,Y., Arora,S., Frank,J. and Johnson,A.W. (2012) Integrity of the P-site is probed during maturation of the 60S ribosomal subunit. *J. Cell Biol.*, **197**, 747–759.

58. Shi,X., Khade,P.K., Sanbonmatsu,K.Y. and Joseph,S. (2012) Functional role of the sarcin-ricin loop of the 23S rRNA in the elongation cycle of protein synthesis. *J. Mol. Biol.*, **419**, 125–138.

59. Wu,S., Tutuncuoglu,B., Yan,K., Brown,H., Zhang,Y., Tan,D., Gamalinda,M., Yuan,Y., Li,Z., Jakovljevic,J. *et al.* (2016) Diverse roles of assembly factors revealed by structures of late nuclear pre-60S ribosomes. *Nature*, **534**, 133–137.

60. Ma,C., Wu,S., Li,N., Chen,Y., Yan,K., Li,Z., Zheng,L., Lei,J., Woolford,J.L. Jr. and Gao,N. (2017) Structural snapshot of cytoplasmic pre-60S ribosomal particles bound by Nmd3, Lsg1, Tif6 and Reh1. *Nat. Struct. Mol. Biol.*, **24**, 214–220.

61. Kater,L., Thoms,M., Barrio-García,C., Cheng,J., Ismail,S., Ahmed,Y.L., Bange,G., Kressler,D., Berninghausen,O., Sinning,I. *et al.* (2017) Visualizing the assembly pathway of nucleolar pre-60S ribosomes. *Cell*, **171**, 1599–1610.

62. Saveanu,C., Namane,A., Gleizes,P.E., Lebreton,A., Rousselle,J.C., Noaillac-Depeyre,J., Gas,N., Jacquier,A. and Fromont-Racine,M. (2003) Sequential protein association with nascent 60S ribosomal particles. *Mol. Cell. Biol.*, **23**, 4449–4460.

63. Pertschy,B., Saveanu,C., Zisser,G., Lebreton,A., Tengg,M., Jacquier,A., Liebminger,E., Nobis,B., Kappel,L., van der Klei,I. *et al.* (2007) Cytoplasmic recycling of 60S preribosomal factors depends on the AAA protein Drg1. *Mol. Cell. Biol.*, **27**, 6581–6592.

64. Panse,V.G. and Johnson,A.W. (2010) Maturation of eukaryotic ribosomes: acquisition of functionality. *Trends Biochem. Sci.*, **35**, 260–266.

65. Clementi,N., Chirkova,A., Puffer,B., Micura,R. and Polacek,N. (2010) Atomic mutagenesis reveals A2660 of 23S ribosomal RNA as key to EF-G GTPase activation. *Nat. Chem. Biol.*, **6**, 344–351.

66. Koch,M., Flür,S., Kreutz,C., Ennifar,E., Micura,R. and Polacek,N. (2015) Role of a ribosomal RNA phosphate oxygen during the EF-G-triggered GTP hydrolysis. *Proc. Natl. Acad. Sci. U.S.A.*, **112**, E2561–E2568.

67. Voorhees,R.M., Schmeing,T.M., Kelley,A.C. and Ramakrishnan,V. (2010) The mechanism for activation of GTP hydrolysis on the ribosome. *Science*, **330**, 835–838.

68. Endo,Y. and Tsurugi,K. (1987) RNA N-glycosidase activity of ricin A-chain. Mechanism of action of the toxic lectin ricin on eukaryotic ribosomes. *J. Biol. Chem.*, **262**, 8128–8130.

69. Stirpe,F. and Battelli,M.G. (2006) Ribosome-inactivating proteins: progress and problems. *Cell. Mol. Life Sci.*, **63**, 1850–1866.

70. Szajwaj,M., Wawiórka,L., Molestak,E., Michalec-Wawiórka,B., Molon,M., Wojda,I. and Tchórzewski,M. (2019) The influence of ricin-mediated rRNA depurination on the translational machinery *in vivo* - New insight into ricin toxicity. *Biochim. Biophys. Acta Mol. Cell. Res.*, **1866**, 118554.

71. Chiou,J.C., Li,X.P., Remacha,M., Ballesta,J.P. and Tumer,N.E. (2008) The ribosomal stalk is required for ribosome binding, depurination of the rRNA and cytotoxicity of ricin A chain in *Saccharomyces cerevisiae*. *Mol. Microbiol.*, **70**, 1441–1452.

72. McCluskey,A.J., Poon,G.M., Bolewska-Pedyczak,E., Srikumar,T., Jeram,S.M., Raught,B. and Gariépy,J. (2008) The catalytic subunit of shiga-like toxin 1 interacts with ribosomal stalk proteins and is inhibited by their conserved C-terminal domain. *J. Mol. Biol.*, **378**, 375–386.

73. DeLano,W.L. (2002) *The PyMol Molecular Graphics System*. DeLano Scientific, San Carlos.

74. Pérez-Cañadillas,J.M., Santoro,J., Campos-Olivas,R., Lacadena,J., Martínez del Pozo,A., Gavilanes,J.G., Rico,M. and Bruix,M. (2000) The highly refined solution structure of the cytotoxic ribonuclease alpha-sarcin reveals the structural requirements for substrate recognition and ribonucleolytic activity. *J. Mol. Biol.*, **299**, 1061–1073.

75. Zhou,Y., Musalgaonkar,S., Johnson,A.W. and Taylor,D.W. (2019) Tightly-orchestrated rearrangements govern catalytic center assembly of the ribosome. *Nat. Commun.*, **10**, 958.